Estimating Unobserved Networks from Heterogeneous Characteristics with an Application to the Swing Riots*

Kieran Marray[1]

[1]Vrije Universiteit Amsterdam and Tinbergen Institute

September 2025

(Link to most recent version)

Abstract

Often, researchers do not observe interactions between individuals that mediate outcomes but do observe rich individual-level characteristics. We present an estimator for unobserved networks from individual outcomes and characteristics that determine who links with whom. The estimator recovers the network by decomposing the covariance matrix of outcomes, penalising possible links differently based on pairwise individual characteristics. We provide theoretical bounds on estimation error, and a fast coordinate descent algorithm that makes estimation tractable for large networks. As an application, we estimate which parishes, distributed across England, rose together during the Swing riots of 1830–1831. We find evidence of a small core of connected uprisings centred on known radical parishes amongst otherwise sporadic unrest. Exposure to different types of uprising polarises elite preferences to expand the right to vote.

Keywords— Networks, graphical lasso, threat of revolution
JEL Codes: C31, D72, D85

1 Introduction

Interactions among economic agents shape a wide range of outcomes. Classmates affect academic performance (Calvó-Armengol et al., 2009; Carrell et al., 2009; Jackson et al., 2022), firm-level shocks propagate through supply chains (Carvalho et al., 2020; Barrot and Sauvagnat, 2016), and information diffuses across villages via informal lending networks (Banerjee et al., 2013). Yet in many cases, the underlying networks of interactions are only partially observed or entirely latent (see Chandrasekhar and Lewis, 2016; Griffith, 2022; Boucher and Houndetoungan, 2025, for a review). To address this, econometricians have begun to develop methods to estimate unobserved links – either decomposing panel data on outcomes generated through the network, (Manresa, 2013; Lam and Souza, 2019; Battaglini et al., 2021; Lewbel et al., 2023; De Paula et al., 2024; Griffith and Peng, 2024), or by imputing the links using structural or statistical models of network formation based on individual characteristics (e.g. Breza et al., 2020).

Here, we introduce an estimator for unobserved links using both panel data on outcomes and characteristics that influence link formation. In our model, outcomes depend on the weighted sum of others'

*We are grateful to Ozan Candogan, Thomas de Graaff, Max Kasy, François Lafond, and seminar participants at the Tinbergen Institute and University of Amsterdam for comments. Further thanks to Josha Dekker for advice optimising the code used in simulations. The usual disclaimer applies.

outcomes through the unknown network (a canonical social interactions model, e.g see Manski, 1993; Battaglini et al., 2021). Individuals with different characteristics interact and form links at different rates. Then, we can estimate the unobserved links by maximising the posterior distribution of links given given the covariance matrix of outcomes and individual characteristics, fixing a set of these interaction rates.[1]

Individual characteristics enter the posterior distribution of links through the prior. We flexibly model link formation using a hierarchical 'spike-and-slab' prior (Ročková and George, 2014; Gan et al., 2019). In the first stage, link probabilities vary with pairwise characteristics. The second stage is a mixture of sparsity-inducing Laplace distributions. The resulting estimator penalises potential links at different rates depending on how frequently individuals with those characteristics interact. Links between types of individuals with higher interaction rates are penalised less heavily. Links between types of individuals with lower interaction rates are penalised more heavily.

As researchers do not know the interaction rates ex-ante, we propose that researchers estimate interaction rates and links simultaneously (Gan et al., 2019). Given a set of interaction rates, the proposed network is given by the maximum a-posteriori estimator for links. To choose interaction rates, the researcher minimises a Bayesian Information criterion over the set of proposed networks (Yuan and Lin, 2007).

Our approach turns the problem of sampling from a complex high-dimensional posterior distribution of links and interaction rates into a tractable two-stage optimisation problem. To solve the inner optimisation problem, we derive a novel coordinate descent algorithm – similar to those in Friedman et al. (2007); Ročková and George (2014); Gan et al. (2019) – that breaks the problem down into a series of regularised linear regression problems solvable by soft-thresholding. The soft-thresholding solution has an intuitive interpretation. We place a link between two individuals if there is a large enough difference between their observed covariance of outcomes and the covariance of outcomes implied by all other indirect paths in the network. The algorithm allows us to tractably estimate large unobserved networks. In simulations, estimating a network with 1000 nodes (100 iterations over $999,000$ possible links) takes an average of 2.25 seconds.

In simulations, the estimator delivers relatively high precision and recall rates for links when $T << N$, and estimated interaction rates are close to true interaction rates. Furthermore, under suitable choice of tuning parameters, our estimator obtains near-optimal error rates, with a constant depending on the number of true links in the network. The error rate extends to a general set of distributions outside of the Gaussian distribution we use to construct the likelihood to construct the posterior distribution of links.

We apply our method to estimate networks of influence between parishes during the 1830-1831 Swing riots in England, and use the estimated networks to test for heterogeneous responses of elite preferences to expand the vote to different revolutionary threats. The Swing riots were a series of uprisings by agricultural labourers, typically regarded as spontaneous responses to declining standards of living and automation of traditional tasks (Hobsbawm and Rudé, 1973; Tilly, 1995; Holland, 2005). There is sparse evidence of labourers agitating for political goals collectively (Hobsbawm and Rudé, 1973; Charlesworth, 1979; Quinault, 1994; Wells, 1997), but no systemic historical evidence remains on how the actions of individual groups of labourers influenced the others (Hobsbawm and Rudé, 1973). We therefore estimate which parishes' risings influenced others. For this, we use covariance in the number of 'large' incidents (machine-breaking, wage riots, expropriation, prisoner rescues, and attacks on law-enforcement) occurring by parish during a seven day rolling window (Tilly, 1995). The number of large riots in a parish depends upon time-invariant local conditions (Caprettini and Voth, 2020), plus the number large incidents within connected parishes.[2] We use geographic distance between parishes as the primary covariate influencing network formation, as in a period without rapid transportation, labourers were more likely to interact locally (Aidt et al., 2022).

We find that few parishes influenced each other, consistent with the thesis of historians that the

[1] In this setting, the maximum a-posteriori estimator with a sparsity-inducing prior for links corresponds to the penalised maximum-likelihood estimator for links from the social interactions model (Battaglini et al., 2021).

[2] We focus on incidents within the week to separate out coordination from the well-documented slow spatial diffusion of rioting north-west from Kent (e.g see Charlesworth, 1979; Aidt et al., 2022).

riots were largely uncoordinated responses to common conditions (Hobsbawm and Rudé, 1973; Tilly, 1995; Holland, 2005). Nonetheless, we find small local networks within the most affected counties, and a concentration of links in the Berkshire-Wiltshire border focussed around parishes like Kintbury – known to historians as "great centres of millitancy in 1830" (Hobsbawm and Rudé, 1973). Parishes that influence, or are influenced by, others are different. They have significantly more incidents of all types of unrest, experienced higher enclosure of common lands, and are more exposed to newspapers.

We use our results to test whether sporadic and coordinated uprisings had different effects on elite support for expanding the right to vote. The 'threat of revolution' theory posits that Western elites extended the franchise to lower orders in response to credible threats of revolution from those groups (Acemoglu and Robinson, 2000, 2001; Aidt and Jensen, 2013). The Swing riots are followed by an election called to settle the question of electoral reform and expanding the right to vote in the United Kingdom. Aidt and Franck (2015) uses exposure to Swing rioting to examine how unrest influenced elite support for reform, proxied by votes for the pro-reform Whigs in that election. We extend this analysis by distinguishing between exposure to general, sporadic unrest and exposure to unrest originating in parishes we estimate to influence others – which we interpret as exposure to more coordinated political action from the lower orders. We find evidence of a polarising effect. Exposure to unrest in general has a larger positive effect on Whig vote share than reported in Aidt and Franck (2015). But, exposure to coordinated unrest has a large negative effect on the vote share for the Whigs conditional on levels of general unrest – evidence of an elite reaction against sharing political power in areas where labourers acted collectively.

On the methodological side, our paper contributes to the growing literature on the econometrics of unobserved or partially observed networks (e.g see Chandrasekhar and Lewis, 2016; Griffith and Peng, 2024; Boucher and Houndetoungan, 2025). While existing works either estimate an unobserved network from panel data of outcomes using a regularised estimator Manresa (2013); Lam and Souza (2019); De Paula et al. (2024); Battaglini et al. (2021); Rose (2023); Lewbel et al. (2023); Griffith and Peng (2024), or impute networks based on characteristics (e.g Breza et al., 2020), our key contribution is to combine both sets of information. Out of these papers, our estimator is closest to the penalised maximum-likelihood estimators in Battaglini et al. (2021); Griffith and Peng (2024), and the estimators in Lubold et al. (2023); Hardy et al. (2024). We further build on the large literature on graphical models in statistics and machine learning (e.g see Wainwright and Jordan, 2008; Janková and Van de Geer, 2018; Gan et al., 2019), particularly Gan et al. (2019)'s Bayesian estimator of links in Markov random fields. Our coordinate-descent approach to solving the optimisation problem for large N parallels the graphical lasso of Friedman et al. (2007). By using Empirical-Bayes methods to reduce a complex sampling problem to an optimisation problem, we follow the nascent literature in 'optimisation-conscious econometrics' (Pouliot, 2023, 2025) and shrinkage methods in econometrics (Fessler and Kasy, 2019; Hansen, 2016).

Our empirical application contributes to the literature in economics and history on the Swing riots and effect of uprisings on elite preferences. Aidt and Franck (2015) are the first to link exposure to the Swing riots to the passage of the Great Reform act, building on a large literature on the impact of threat of revolution on franchise expansions (e.g see Acemoglu and Robinson, 2000, 2001; Conley and Temimi, 2001; Aidt and Jensen, 2013). Caprettini and Voth (2020) link incidents of rioting to parish-level conditions. Our use of distance to predict contagion of unrest between parishes builds on Aidt et al. (2022), who study the slower diffusion of incidents of rioting across England over multiple weeks. Within the historical literature, Hobsbawm and Rudé (1973); Charlesworth (1979); Tilly (1995); Holland (2005) conduct detailed surveys of the causes, progress, and impact of the Swing riots.

Outline First, in Section 2, we set up our econometric problem. Section 3, derives our estimator, its theoretical properties, and describes the algorithm we use to implement the estimator. Finally, in Section 4 we apply our estimator to the Swing riots. All proofs are given in the appendix.

2 Setup

Consider a researcher who observes a set $\mathcal{N} = \{1, ..., N\}$ of individuals across T time periods. The number of individuals N is fixed such that $N > T$. The individuals are connected on a weighted, simple network

with adjacency matrix G. Individual outcomes y_{it} depend on others outcomes y_{jt} through the network of connections G, covariates x_{it}, and idiosyncratic shocks ϵ_{it} by the data generating process (Battaglini et al., 2021)

$$y_{it} = \sum_j G_{ij} y_{jt} + x_{it}\beta + \epsilon_{it} \tag{1}$$

– a common model in the literature on spatial and network econometrics (e.g see De Paula, 2017).

The researcher observes $\{y_{it}, x_{it}\}_{i\in\mathcal{N},t=1,...,T}$ and covariates $\{x_{it}\}_{i\in\mathcal{N},t=1,...,T}$, wants to estimate the weighted adjacency matrix G – how much each individual affects each other.

We assume that the network is formed in a process that we can describe in three steps. First, nature draws each individual i some M-dimensional vector of characteristics $z_i \in \mathbb{Z}^M$. Without loss of generality, we let these be discrete categories. Second, pairs of individuals form connections at rates that depend on their pairwise characteristics. Let A denote a binary matrix where

$$G_{ij} \neq 0 \text{ only if } A_{ij} = 1 \tag{2}$$

i.e A measures which pairs of individuals interact. Formally, A is one draw from a random graph generating process $\mathcal{A}(Z, \eta)$ with the vector of interaction rates $\eta \in [0, 1)^{M^2}$

$$\eta = \begin{pmatrix} \eta_{z_1,z_1} & \eta_{z_1,z_2} & ... & \eta_{Z_M,Z_M} \end{pmatrix}$$

such that

$$A_{ij}|(z_i, z_j) \sim \text{Bernoulli}(\eta_{z_i,z_j}). \tag{3}$$

We assume that η is not known to the researcher ex-ante. Third, given that two individuals are connected ($A_{ij} = 1$), they interact with some time-invariant intensity $G_{ij} > 0$.

This reduced-form network formation model is a plausible in many economic settings. For example, we may model individuals in villages forming links at rates that depend on which village each is from (Banerjee et al., 2013). Children in schools may form links at different rates depending on each child's gender (Currarini et al., 2009). Alternatively, firms from different municipalities may search for suppliers across space at different rates depending their municipalities (Arkolakis et al., 2023). In the appendix, we show that this structure can be microfounded as the equilibrium outcome of a game on a network with linear quadratic utilities and individual-specific consideration sets (Calvó-Armengol et al., 2009; Abaluck and Adams-Prassl, 2021). If we consider the power set of possible $\mathbb{Z}^M$ as communities, we can think of our network formation model as a non-parametric approximation to a continuous underlying network formation process (Airoldi et al., 2013).[3]

Our specification imposes several noteworthy restrictions on our data. Firstly, links on the network do not change over time (similar to De Paula et al., 2024; Lewbel et al., 2023). This rules out endogenous effects where individuals adjust links over time in response to spillovers (e.g see König et al., 2019). Second, all interactions have the same sign. Third, unlike De Paula et al. (2024) we do not allow for a direct effect of covariates on neighbours' outcomes through the network.[4] The effect of one individual's covariates on others' outcomes only comes through the effect on the individual's own outcomes. This assumption is appropriate for our empirical example in Section 4.

We impose four following assumptions on this data generating process. To start with, we assume that all non-zero entries are 'large enough'.

Assumption 1. Minimum detectable entry size

$$min\{G_{ij}|G_{ij} \neq 0\} > c\sqrt{\frac{\ln N}{T}}$$

[3]Instead, we could let the network formation process be more general by instead parameterising η as a continuous function of underlying characteristics Z. An example of this might be exponential decay of interaction probabilities in distance.

[4]Our estimator could be extended to this case in the case of fixed covariates. We focus on a single estimator for simplicity.

for some constant $c > 0$.

As the number of time periods gets smaller, or the number of individuals gets larger, the smallest present link must get stronger. In practice, this tells us the size of the smallest detectable link. As the number of possible links gets larger relative to time periods, it gets harder to distinguish the presence of the link from noise.

Second, as is standard in the spatial and network econometric literature, the network must have a spectral radius less than 1 (Battaglini et al., 2021),

Assumption 2. Spectral radius – $\rho(G) < 1$,

and we assume for simplicity that any covariates are deterministic

Assumption 3. Deterministic covariates – x_{it} are uniformly-bounded, deterministic variables for all i.

Finally, as standard in the literature on graphical models (e.g see Wainwright and Jordan, 2008; Janková and Van de Geer, 2018; Gan et al., 2019) we assume that errors are independently and identically distributed from a Normal distribution with parameter $\sigma^2 > 0$.

Assumption 4. Distribution of errors – $\epsilon_t \sim N(0, \sigma^2 I)\ \forall t$.

This allows us to write down our likelihood function for links given. In practice, we can relax the assumption that the distribution in Gaussian. Indeed, our theoretical guarantees on estimation accuracy apply to general distributions with exponential and polynomial tails (see Section 3). Our estimator will attribute homoskedasticity in errors across nodes that we cannot account for by covariates to links between individuals in the latent network. For relaxations of this, see Griffith and Peng (2024).

For estimation, we will work with the component of y_{it} that varies orthogonally to x_{it}. Define the projection matrix

$$P_x = x(x'x)^{-1}x'.$$

Stacking each individual's outcomes y_{it} into $T \times 1$ vector y_t, we project out the effect of covariates

$$(I - P_x)y_t.$$

and stack the resulting outcomes into the $T \times N$ matrix Y. Under Assumption 4, we can describe these outcomes as being normally distributed

$$Y \sim N(0, \sigma^2((I - G)(I - G)')^{-1}). \tag{4}$$

The unobserved networks enters through the covariance of outcomes. Under assumption 2, we can rewrite

$$(I - G)^{-1} = \sum_{k=0}^{\infty} G^k$$

– the matrix encoding all paths of any given length between any two individuals on the network. So the covariance of two individuals' outcomes depends on the variance of shocks and the number of paths of any length between them.[5]

[5] An alternative way of stating this is that our outcomes can be described by a Markov random field parameterised by the precision matrix

$$\begin{aligned}\Theta &= \frac{1}{\sigma^2}(I - G)(I - G)' \\ &= \frac{1}{\sigma^2}(I - 2G + GG')\end{aligned}$$

that encodes the conditional independence structure between the series of individual level outcomes Y (Janková and Van de Geer, 2018). Two individuals' outcomes are independent of each other conditional on all other outcomes if there are no links of up length two between them.

3 Estimation

Consider the problem of jointly estimating links G, the variance of shocks σ^2, and interaction rates η from the posterior distribution of G, σ^2 given outcomes Y, characteristics Z, and η. As data, we construct the sample covariance matrix of outcomes across individuals S such that

$$S_{ij} = \frac{1}{T}\sum_{t=1}^{T} Y_{it}Y_{jt}.$$

Our main result is that we can formulate this estimation problem as a two-stage optimisation problem, where the inner stage is convex conditional on estimated interaction rates. This allows us to bound the error of the estimated network from the true network, and to derive an algorithm to tractably estimate moderately-sized networks.

3.1 Objective function

To construct the posterior distribution of links and the variance of shocks given interaction rates and our data, we need to formulate a likelihood for the network and variance given outcomes, and priors for both given characteristics and interaction rates. From the distribution of outcomes (4), it follows that the log-likelihood of outcomes Y given the network of connections G and variance σ^2 is

$$l(G, \sigma^2) = \log\det\Big(\frac{(I-G)(I-G)'}{\sigma^2}\Big) - \operatorname{trace}\Big(S\frac{(I-G)(I-G)'}{\sigma^2}\Big). \tag{5}$$

Given our network generating process, we can model the off-diagonal elements of the adjacency matrix using a 'spike-and-slab' prior (Ročková and George, 2018; Gan et al., 2019).

$$\begin{aligned}\pi(G_{ij}) &= p(A_{ij}=1|z_i,z_j)\frac{1}{2\nu_1}e^{\frac{-|G_{ij}|}{\nu_1}} + p(A_{ij}=0|z_i,z_j)\frac{1}{2\nu_0}e^{\frac{-|G_{ij}|}{\nu_0}} \\ &= \frac{\eta_{z_i,z_j}}{2\nu_1}e^{\frac{-|G_{ij}|}{\nu_1}} + \frac{1-\eta_{z_i,z_j}}{2\nu_0}e^{\frac{-|G_{ij}|}{\nu_0}}.\end{aligned} \tag{6}$$

More intuitively, we can express this as the hierarchical prior

$$\begin{aligned}\pi(G_{ij}) &= \begin{cases} p(G_{ij}|A_{ij}=0) & \sim \text{Laplace}(0,\nu_0) \\ p(G_{ij}|A_{ij}=1) & \sim \text{Laplace}(0,\nu_1)\end{cases} \\ A_{ij}|z_i,z_j &= \text{Bernoulli}(\eta_{z_i,z_j}).\end{aligned}$$

The first level of the prior models the presence of links between individuals at different rates η_{z_i,z_j} depending on individual characteristics z_i, z_j. The second level then models the entries of the adjacency matrix given the presence or not of a link. Here, we use a mixture of Laplace priors – one prior for individuals that are connected, and one for those that are not.[6] Figure 1 plots an example of these distributions. In our case, the penalty will force links that explain little of the covariance in outcomes to zero. In addition to η, which we will estimate, our spike-and-slab prior is parameterised by the scale parameters for the two Laplace distributions ν_0, ν_1. Setting $\nu_1 > \nu_0$ means that there is more likely to be a non-zero entry of the adjacency matrix if we predict that there is a link between individuals than if we do predict that there is a link between individuals. As a prior for σ^2, we use the uniform prior

$$f(\sigma^2) = U(0, \sigma^2_{\max}) \tag{7}$$

where we set $\sigma^2_{\max}$ below the observed variance of the data.

[6]Maximum a-posteriori estimation with a Laplace prior is equivalent to the standard l1 penalised maximum likelihood estimator or graphical lasso algorithm (Gan et al., 2019; Friedman et al., 2007). Including some form of penalty is necessary for identification of our subsequent estimator in the case where $N > T$ – see Battaglini et al. (2021).

Figure 1: Example 'spike-and-slab' prior

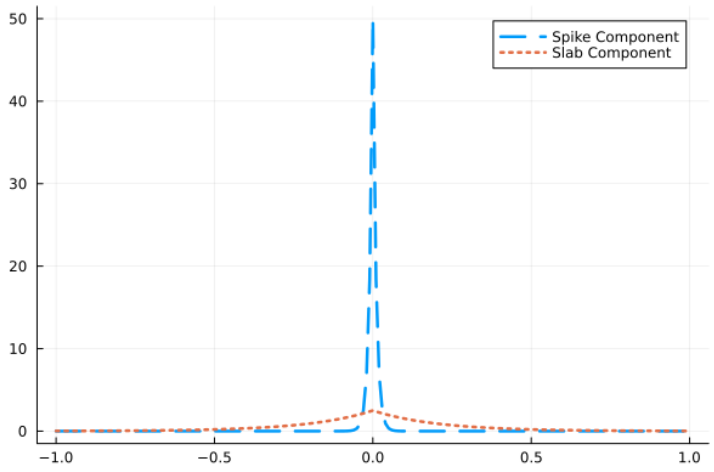

Notes: Example for parameters $v_0 = 1/100, v_1 = 1/5$.

Given our priors and likelihood, we can jointly estimate G and η from the posterior distribution by a form of empirical Bayes (Gan et al., 2019; Fessler and Kasy, 2019). First, consider estimation of G, σ^2 for fixed η^*. Using Eqs. 5, 6, and 7, we can write the logarithm of the posterior distribution as

$$\begin{aligned} L(G, \sigma^2 | Y, Z, \eta^*) &= \ln \pi(G, \sigma^2 | Y, Z, \eta^*), \\ &= l(G, \sigma^2) + \sum_{i,j} \ln \pi(G_{ij} | z_i, z_j, \eta^*) + \text{ const}, \\ &= \log \det\Big(\frac{(I-G)(I-G)'}{\sigma^2}\Big) - \text{trace}\Big(S\frac{(I-G)(I-G)'}{\sigma^2}\Big) \\ &+ \sum_{i,j} \ln\Big(\frac{\eta^*_{z_i,z_j}}{2\nu_1} e^{-\frac{|G_{ij}|}{\nu_1}} + \frac{1-\eta^*_{z_i,z_j}}{2\nu_0} e^{-\frac{|G_{ij}|}{\nu_0}}\Big) + \text{ const}, . \end{aligned} \tag{8}$$

We take the maximum a-posteriori estimators $\hat{G}(\eta^*), \sigma^2(\eta^*)$. Dropping the constant, the estimates maximise the objective function

$$\begin{aligned} L(G, \sigma^2 | Y, Z, \eta^*) &= \log \det\Big(\frac{(I-G)(I-G)'}{\sigma^2}\Big) - \text{trace}\Big(S\frac{(I-G)(I-G)'}{\sigma^2}\Big) \\ &+ \sum_{i,j} \ln\Big(\frac{\eta^*_{z_i,z_j}}{2\nu_1} e^{-\frac{|G_{ij}|}{\nu_1}} + \frac{1-\eta^*_{z_i,z_j}}{2\nu_0} e^{-\frac{|G_{ij}|}{\nu_0}}\Big) \end{aligned}$$

This is a natural estimator for G, σ^2 as it corresponds to the usual penalised maximum-likelihood estimator (e.g see Friedman et al., 2007; Battaglini et al., 2021) except, instead of imposing a constant penalty on the occurrence of each link, it more heavily penalises links that less likely to occur based individual characteristics. To see this consider the subgradient of our penalty term above with respect to a link G_{ij}

$$\partial_{G_{ij}} \ln \pi(G_{ij} | z_i, z_j, \eta^*) = p(A_{ij} = 1 | \eta^*_{z_i,z_j}) \frac{1}{\nu_1} + (1 - p(A_{ij} = 1 | \eta^*_{z_i,z_j})) \frac{1}{\nu_0}.$$

The subgradient of the penalisation term is the average of two penalisation terms weighted by the conditional probabilities a link is present or not given characteristics and estimated interaction rates (Gan et al., 2019). Through setting $\nu_1 > \nu_0$, we penalise links more between individuals that are less likely connected based on characteristics (more heavily weighting the 'spike' of the mixture distribution),

and less between those that we think are more likely to be present based in characteristics (more heavily weighting the 'slab' of the mixture distribution).

In practice, we need to impose our assumptions on the spectral radius of the adjacency matrix, and that there are no self loops. Adding these constraints alongside Eq. 8 gives the constrained optimisation problem

$$\begin{aligned}\hat{G}(\eta), \hat{\sigma}^2(\eta) = &\max_{G_{ij}>0, \sigma^2 \in [0, \sigma^2_{\max}]} \log\det\Big(\frac{(I-G)(I-G)'}{\sigma^2}\Big) - \text{trace}\Big(S\frac{(I-G)(I-G)'}{\sigma^2}\Big) \\ &+ \sum_{i,j} \ln\Big(\frac{\eta^*_{Z_i,z_j}}{2\nu_1} e^{-\frac{|G_{ij}|}{\nu_1}} + \frac{1-\eta^*_{Z_i,z_j}}{2\nu_0} e^{-\frac{|G_{ij}|}{\nu_0}}\Big) \\ &\text{s.t } \rho(G) < 1, G_{ii} = 0 \ \forall i.\end{aligned} \tag{9}$$

Given the inner problem 9, we can then solve for the interaction rates η given the estimates of $\hat{G}(\eta), \sigma^2(\eta)$. Following Gan et al. (2019), we pick η^* to minimise the Bayesian Information Criterion for high-dimensional covariance matrix estimators of Yuan and Lin (2007)

$$\begin{aligned}\eta^* = \min_{\eta} &- n\Big(\text{trace}\Big(S\frac{(I-\hat{G}(\eta))(I-\hat{G}(\eta))'}{\hat{\sigma}^2(\eta)}\Big) - \log\det\Big(\frac{(I-\hat{G}(\eta))(I-\hat{G}(\eta))'}{\hat{\sigma}^2(\eta)}\Big)\Big) \\ &+ \ln(n) \times |\{\hat{G}_{ij}(\eta) : \hat{G}_{ij}(\eta) \neq 0\}|.\end{aligned}$$

3.2 Theoretical properties

First, we note that the inner optimisation problem Eq. 9 is convex.

Proposition 1. Assume that $\nu_1 > \nu_0$ and $\eta_{z_i,z_j} \in [0,1)\ \forall i,j$. Then, the optimisation problem Eq. 9 is convex with respect to $G_{ij}\ \forall i \neq j$.

This tells us that, for a fixed set of interaction rates η, the adjacency matrix of the network G is identified.

Next, we want to bound the distance of the estimate from the true network. Let $\hat{G}$ denote the solution to the inner optimisation problem. We can show that the estimated network is close to the true network.

Theorem 1. Define $a = ||A||_\infty$, and denote $M_{B^0} = |||B^0|||_\infty$. Define

$$\Gamma = ((I-G)'(I-G))^{-1} \otimes ((I-G)'(I-G))^{-1}, M_A = |||A^{-1}|||_\infty.$$

Make assumptions 1, 2, 3 plus the assumptions that

$$\begin{aligned}\frac{1}{T\nu_0} &> C_4\sqrt{\frac{\ln N}{T}}, \\ \frac{1}{T\nu_1} &> C_3\sqrt{\frac{\ln N}{T}}, \\ \frac{\nu_1^2(1-\eta_{ij})}{\nu_0^2\eta_{ij}} &\leq N^\iota\ \forall i,j, \text{ and} \\ \sqrt{T} &\geq Ca\sqrt{N}\end{aligned}$$

for some constants C_3, C_4 s.t $C_4 > C_3 > 0$, small ι, and $C = 2(2C_1 + C_2)M_{\Gamma_0}\max(3M_{\Sigma_0}, 3M_{\Gamma_0}M^3_{\Sigma_0})$.

If ϵ is from a distribution with exponential tails i.e there exist some $\gamma, c_1 > 0, N \leq c_1 T^\gamma$, and for some $\delta_0 < 0$

$$E|\epsilon_i|^{4\gamma+4+\delta_0} \leq K\ \forall i = 1, ..., N,$$

then

$$||\hat{G} - G||_F \leq 2(2C_1 + C_3)M_{\Gamma_0}\sqrt{\frac{a \ln N}{T}}.$$

where

$$C_1 = a^{-1}(2 + \tau_0 + a^{-1}K^2)$$

with probability greater than $1 - 2N^{-\tau_0}$.

If we instead assume that ϵ is from a distribution with polynomial tails i.e there exist some $\gamma, c_1 > 0, N \leq c_1 T^{\gamma}$, and for some $\delta_0 < 0$

$$E|\epsilon_i|^{4\gamma+4+\delta_0} \leq K \ \forall i = 1, ..., N,$$

then

$$||\hat{G} - G||_F \leq 2(2C_1 + C_3)M_{\Gamma_0}\sqrt{\frac{a \ln N}{T}}.$$

where

$$C_1 = \sqrt{(\Theta_{\max} + 1)(4 + \tau_0)}$$

with probability greater than $1 - O(T^{-\frac{\delta_0}{8}} + N^{-\frac{\tau_0}{2}})$.

Note that the necessary sample size depends on the maximum row sum of A, which itself depends on the characteristics Z. This theorem tells us that if number of possible connections for nodes in the network is sparse due to underlying characteristics – the rate $\eta_{ij} = 0$ for most i, j – then we can detect networks with a very small T relative to N. As the set of possible links gets larger and larger, and interaction rates get higher, we need larger T to detect the true network for a given N.

3.3 Implementation

To implement the estimator, we need to solve the constrained optimisation problem Eq. 9. This type of problem is hard to solve in practice (Ročková and George, 2014; Gan et al., 2019). So, here we derive an EM algorithm to efficiently solve Eq. 9 for large N. Recall that we can write the log of the prior (our regularisation term in Eq. 9) in terms of the matrix of connections A as

$$\sum_{ij} \ln \Big(p(A_{ij} = 1|z_i, z_j)\frac{1}{2\nu_1}e^{\frac{-|G_{ij}|}{\nu_1}} + p(A_{ij} = 0|z_i, z_j)\frac{1}{2\nu_0}e^{\frac{-|G_{ij}|}{\nu_0}} \Big).$$

To solve Eq. 9, we sample A as a latent variable alongside G, fixing σ^2 (Ročková and George, 2014). Then, we can solve for estimates of G maximising the expected likelihood given A (Gan et al., 2019). Finally, we can solve for σ^2 by maximising the posterior distribution over the resulting estimates.

First, note that we can rewrite the joint log-posterior distribution Eq. 8 as

$$L(G, \sigma^2, A|Y, Z, \eta) = l(G, \sigma^2) + \sum_{ij} \ln \left(P(A_{ij}|\eta, z_i, z_j)p(G_{ij}|A_{ij}) \right) + \text{const.}$$

Let P denote the matrix such that

$$\begin{aligned} P_{ij} &= E(A_{ij}) \\ &= p(A_{ij} = 1|z_i, z_j). \end{aligned}$$

In the E step, we can sample P given estimated G^k as in Gan et al. (2019)

$$\ln \frac{P_{ij}}{1 - P_{ij}} = \ln \frac{\nu_0}{\nu_1} + \ln \frac{\eta_{z_i,z_j}}{1 - \eta_{z_i,z_j}} - \frac{|G^k_{ij}|}{\nu_1} + \frac{|G^k_{ij}|}{\nu_0}. \tag{10}$$

Then, we can write the expectation of log-posterior over A as

$$\begin{aligned} Q(G|G^k) = \log\det\Big(\frac{(I-G)(I-G)'}{\sigma^2}\Big) - \mathrm{trace}\Big(S\frac{(I-G)(I-G)'}{\sigma^2}\Big) \\ + \sum_{i,j} P_{ij}(-\ln 2\nu_1 - \frac{|G_{ij}|}{\nu_1} + \ln \eta_{z_i,z_j}) \\ + \sum_{i,j}(1-P_{ij})(-\ln 2\nu_0 - \frac{|G_{ij}|}{\nu_0} + \ln(1-\eta_{z_i,z_j})). \end{aligned}$$

Maximising this gives us our estimate G^{k+1}. To solve for $\hat{G}, \hat{A}$, we can iterate until convergence.

Maximising the $Q()$ function over for a complete (simple) network G^k involves simultaneously estimating $N(N-1)$ parameters. As this scales quadratically in N, this becomes difficult to directly optimise for even small N. As a solution, we propose a network lasso algorithm inspired by the graphical lasso of (Friedman et al., 2007). This allows us to break this hard non-linear optimisation problem into a series of lasso problems that we can solve iteratively using a soft-thresholding algorithm. The soft-thresholding algorithm is relatively fast, allowing us to solve relatively large problems with thousands of individuals.

Taking subdifferentials of our $Q()$ function with respect to G gives the first-order condition

$$-\frac{2}{\sigma^2}S(I-G) + 2(I-G)^{-1} - \Gamma = 0,$$

where the matrix Γ encodes the subdifferentials of the penalty function with respect to each G_{ij}

$$\Gamma_{ij}\begin{cases} \in [-(\frac{1}{\nu_1}P_{ij} + \frac{1}{\nu_0}(1-P_{ij})), (\frac{1}{\nu_1}P_{ij} + \frac{1}{\nu_0}(1-P_{ij}))] & \text{if } G_{ij} = 0 \\ = (\frac{1}{\nu_1}P_{ij} + \frac{1}{\nu_0}(1-P_{ij})) & \text{if } G_{ij} > 0. \end{cases}$$

for $i \neq j$. Rearranging, we have

$$2(S - \sigma^2(I-\gamma G)^{-1} - SG) - \sigma^2\Gamma = 0.$$

Consider the i,jth entry of this matrix condition. We have

$$2(S_{ij} - \sigma^2(I-G)^{-1}_{ij} - S_{ii}G_{ij} - \sum_{k\neq j} S_{i,k}G_{k,j}) - \sigma^2\Gamma_{ij} = 0.$$

– which we recognise as a Lasso problem (Tibshirani, 1996). Rearranging for G_{ij} gives

$$G_{ij} = \frac{1}{S_{ii}}(S_{ij} - \sum_{k\neq j} S_{i,k}G_{k,j} - \sigma^2(I-G)^{-1}_{ij} - \frac{1}{2}\sigma^2\Gamma_{ij}).$$

Therefore we can solve for G_{ij} column-wise using an iterative soft-thresholding algorithm (Friedman et al., 2010). Denote

$$\rho_{ij} = S_{ij} - \sum_{k\neq j} S_{i,k}G_{k,j} - \sigma^2(I-G)^{-1}_{ij}.$$

The updating rule for each G_{ij} is

$$G_{ij} = \begin{cases} \frac{\rho_{ij} - \frac{1}{2}\sigma^2\Gamma_{ij}}{S_{ii}} & \text{if } \rho_{ij} > \frac{1}{2}\sigma^2 Z_{ij}, \\ 0 & \text{if } \rho_{ij} \leq \frac{1}{2}\sigma^2\Gamma_{ij}. \end{cases}$$

An additional complication is updating the inverse $(I-G)^{-1}$ after estimating each column, which would be computationally expensive. However, we can use that for a rank-one update to a matrix that we can write as the outer product of two vectors uv', the inverse is computable as (Sherman and Morrison, 1949)

$$((I-G)+uv')^{-1} = (I-G)^{-1} - \frac{(I-G)^{-1}uv'(I-G)^{-1}}{1+v'(I-G)^{-1}u}.$$

Writing

$$u = -(G_{12}^k - G_{12}^{k-1})$$
$$v = e_2 \text{ the unit basis vector,}$$

we can write each new column estimate as a rank-one update to $I-G$, uv', and apply this rule within our algorithm.

The full algorithm we use to solve the inner optimisation problem is given in Alg. 1. To test the speed of our algorithm, we time 100 single loops with a moderately sized network of $N = 1000$ (optimising over $999,000$ variables). The mean execution time is 2.55 seconds.

Algorithm 1 Network lasso

procedure BLOCK COORDINATE DESCENT($S, G_0, \sigma^2, \nu_0, \nu_1, \delta$)
  $G \leftarrow G_0$
  $\Lambda = (I - G_0)^{-1}$
  while $||G^k - G^{k-1}||_F \geq \delta$ **do**
    $G^k \leftarrow G^{k-1}$.
    for $i, j \in 1, ..., N$ **do**
      $P_{ij} = \left(1 + \frac{\nu_1}{\nu_0} e^{-\frac{|G_{ij}^k|}{\nu_0} + \frac{|G_{ij}^k|}{\nu_1}} \frac{1-\eta_{z_i,z_j}}{\eta_{z_i,z_j}}\right)^{-1}$
    end for
    for $i \in 1, ..., N$ **do**
      $v = e_i$
      for $j \in 1, ..., N$ **do**
        $\Gamma_{ij} = P_{ij}\frac{1}{\nu_1} + (1 - P_{ij})\frac{1}{\nu_0}$
        $\rho_{ij} = S_{ij} - \sum_{;\neq j} S_{i,l} G_{l,j}^k - \sigma^2 \Lambda_{ij}$.
        $G_{ij}^k = \begin{cases} 0 & \text{if } \rho_{ij} \leq \frac{1}{2}\sigma^2\Gamma_{ij}, \\ \frac{\rho_{ij} - \frac{1}{2}\sigma^2 Z_{ij}}{S_{ii}} & \text{if } \rho_{ij} > \frac{1}{2}\sigma^2\Gamma_{ij}. \end{cases}$
      end for
      $u = -(G_{:,j}^k - G_{:,j}^{k-1})$
      $\Lambda = \Lambda - \frac{\Lambda u v' \Lambda}{1 + v'\Lambda u}$.
    end for
    $i \leftarrow i + 1$
  end while
  Return G^k.
end procedure

Using the results in Tseng (2001), we can show that the result of this algorithm converges to the true maximiser of the inner optimisation problem

Proposition 2. Make assumptions 1 and 2. Let $\hat{G}^k$ denote the k-th estimate from Alg. 1 and G^* denote the maximiser of the inner optimisation problem Eq. 9 fixing η, σ^2. As $k \to \infty$, $\hat{G}^k \to G^*$.

To solve for σ^2, we simply maximise the posterior distribution over the results of this algorithm. Having solved the inner optimisation problem fixing η, we have to determine the interaction rates η plus the regularisation parameters ν_1, ν_0. To estimate η, we minimise the BIC over the maximum a-posteriori estimates of G given η, ν_0, ν_1. Unfortunately, we have no theoretical guarantees that our outer problem is convex with a unique global minimum.[7]. Therefore, we recommend estimating η, ν_0, ν_1 by a form of

[7]Indeed, in simulations we can generate cases where there are multiple local minima.

global optimisation enforcing that $\nu_1 > \nu_0$. In practice, we apply a local grid search strategy to sweep the parameter space. This works well in practice for low-dimensional η. Further research could explore more efficient strategies when the dimension of η becomes larger.

Algorithm 2 Full estimation algorithm

procedure GRID SEARCH($\mathcal{H}, \Sigma, G_0, S, \nu_0, \nu_1, \delta$)
  for $\eta \in \mathcal{H}$ **do**
    $\hat{G}(\eta), \hat{\sigma}^2(\eta) = \text{argmax}_{\sigma^2 \in \Sigma}\{L(\text{Network Lasso}(\eta, G_0, S, \delta), \sigma^2)\}$

$$\text{BIC}(\eta) = -n\Big(\text{trace}\Big(S\frac{(I - G^*(\eta))(I - G^*(\eta))'}{\hat{\sigma}^2}\Big) + \log\det\Big(\frac{(I - G^*(\eta))(I - G^*(\eta))'}{\hat{\sigma}^2}\Big)\Big) + \ln(n) \times |\{G^*_{ij}(\eta) : G^*_{ij}(\eta) \neq 0\}|$$

  end for
  $\hat{\eta} = \text{argmin}_{\eta \in \mathcal{H}}\{\text{BIC}(\eta)\}$
  $\hat{G}, \hat{\sigma}^2 = \hat{G}(\hat{\eta}), \hat{\sigma}^2(\hat{\eta})$.
end procedure

3.4 Simulations

In addition to our theoretical guarantees, we assess the finite sample performance of our estimates in simulation. As our unobserved networks, we simulate the interaction of individuals across parishes. Nodes are partitioned into M blocks $Z_1, ..., Z_M$ (parishes). The latent network of interations A is a drawn randomly such that nodes form links at a certain rate within blocks, and a certain rate between blocks.

$$A_{ij}|z_i = z_j \sim \text{Bernoulli}(\eta_1),$$
$$A_{ij}|z_i \neq z_j \sim \text{Bernoulli}(\eta_2).$$

Given a sampled A, we set interaction intensities by row-normalising the matrix of connections

$$G_{ij} = \frac{A_{ij}}{\sum_j A_{ij}}$$

to generate the network of interaction intensities G. Given a sampled G, we then simulate outcomes from the model

$$Y_{it} = (I - G)^{-1}\epsilon_{it}$$

for $t = \{1, ..., T\}$ with $\epsilon_{it} \sim$ i.i.d $N(0, 1)$ for ease.[8] We set $T < N$ in each case, and vary the ratio $\frac{N}{T} \in \{2, 3, 6, 12\}$. To estimate η, we use a local grid search.

We consider four different measures of the quality of our estimates

1. Precision – the total number of true links detected divided by the total number of estimated links on the network
$$\text{Precision} = \frac{\sum_{ij} \mathbf{1}(\hat{G}_{ij} > 0)\mathbf{1}(G_{ij} > 0)}{\sum_{ij} \mathbf{1}(\hat{G}_{ij} > 0)}$$
2. Recall – the total number of true links detected divided by the total number of true links on the network

[8] We get results that are quantitatively similar when jointly estimating σ^2.

$$\text{Recall} = \frac{\sum_{ij} \mathbf{1}(\hat{G}_{ij} > 0)\mathbf{1}(G_{ij} > 0)}{\sum_{ij} \mathbf{1}(G_{ij} > 0)}$$

3. The distance between the estimated network and true network

$$||\hat{G} - G||_F.$$

4. The estimates $(\hat{\eta}_1, \hat{\eta}_2)$.

Outcomes are computed by averaging over 100 draws of $G, \{\epsilon_{it}\}_{i,t}$.

Table 1: Performance of estimator on simulated networks

N	T	Precision	Recall	Distance	$\hat{\eta_1}$	$\hat{\eta_2}$
300	150	0.75	0.90	7.07	0.28	0.05
300	100	0.71	0.850	7.40	0.32	0.05
300	50	0.63	0.76	8.02	0.28	0.041
300	25	0.45	0.63	8.93	0.28	0.065

Notes: Results averaged over 100 simulated networks and errors. 'Distance 'is Frobenius norm of the difference between the true and estimated network. The number of blocks is kept constant at $\frac{N}{10}$.

Precision and recall are high when T is relatively high compared to N. As T falls, performance falls as well. However with T very small relative to N, recall remains relatively high. In all cases, distance between estimated and true matrices are fairly low. Estimates of interaction rates also remain reasonably close to true interaction rates.

4 Application: networks of unrest during the Swing riots

As an application, we estimate how rioting in different parishes influenced others during the Swing riots of 1830-1831. We then use the results of the 1831 general election in nearby constituencies to test for heterogeneous effects of exposure to different types of unrest on elite preferences to extend the right to vote.

4.1 The Swing riots of 1830–1831

The Swing riots were a series of uprisings by landless labourers concentrated in southern England between August 1830 and February 1831 – the largest rural unrest in 19th century England (Tilly, 1995). At the time, agriculture was dominated by medium and large farms employing a large mass of landless agricultural labourers in seasonal work. Economic and social changes, including enclosure of common land and automation of traditional work, eroded traditional life and immiserated many labourers (Hobsbawm and Rudé, 1973). Poor harvests and automation of seasonal work sparked unrest (Hobsbawm and Rudé, 1973; Holland, 2005). Risings began in Kent on June 28th 1830, with labourers burning barns, breaking machines, and demanding compensation from landowners – often preceded by threatening letters signed by a mysterious "Captain Swing" (Holland, 2005).

Uprising diffused slowly North and West through roads and local communication networks (see Charlesworth, 1979; Aidt et al., 2022). Authorities struggled to contain unrest (Hobsbawm and Rudé, 1973; Holland, 2005), raising the spectre of an English revolution similar to the contemporaneous revolutions France and Belgium. (Aidt and Franck, 2015) finds evidence that the rioting led to a subsequent expansion of the right to vote due to fear of revolution.

Figure 2: Swing incidents in England 1830–31

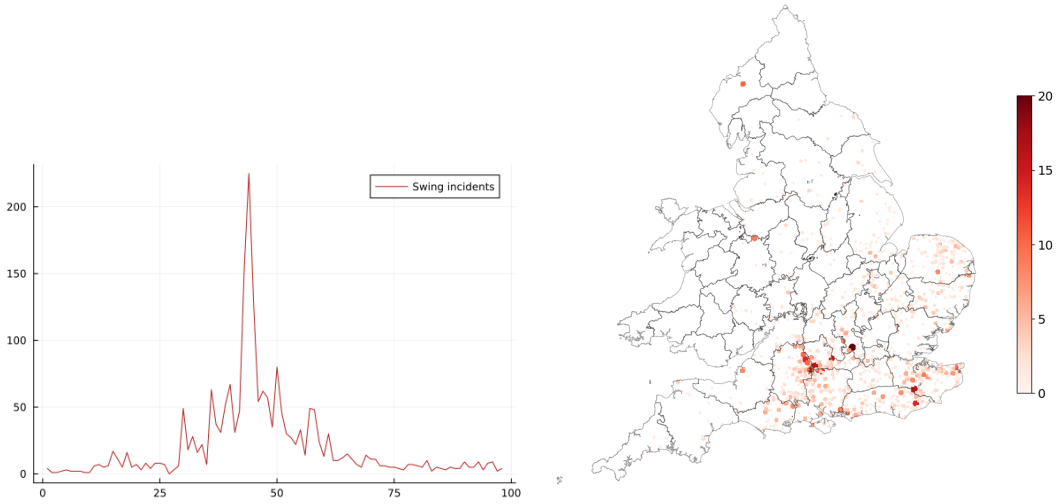

(a) Incidents by day, June 1830–February 1831

(b) Distribution of incidents by parish – size/colour denotes number of riots

We estimate how risings in parishes influenced others in the short term, separate from the slower spatial diffusion of risings, to distinguish between two forms of protest: localised responses to parish-specific social conditions (which has a long history in the English countryside Hobsbawm and Rudé, 1973), and broader agitation rooted in shared grievances of agricultural labourers as a group.

There is evidence of both during the riots (Charlesworth, 1979; Quinault, 1994; Wells, 1997). While most rioting took the form of traditional rural protest – sporadic incendarism – there were signs of political mobilization amongst the labourers. There is evidence that small cores of politicised labourers drove unrest (Charlesworth, 1979), and that many were aware of and supported the revolutions abroad (Quinault, 1994). Records remain of politicised workers organizing joint demands for compensation, as in Hungerford and Kintbury in Berkshire, where:

"Other villages, whose inhabitants had no doubt heard of the outcome of the Hungerford confrontation, sent a deputation that night to join the Kintbury labourers to invite them to join in combined operations. So the next day the riots continued ..." (Hobsbawm and Rudé, 1973, pg. 138)

Labourers even met to demand electoral reform, and a letter signed by "Captain Swing" was sent to the Prime Minister demanding it (Holland, 2005).

Contemporaries worried about this sort of agitation amongst the agricultural workers. One magistrate is recorded to have warned the Home Secretary, Sir Robert Peel, that the rioting would lead

" the Peasantry [to] learn the secret of their own physical strength."(Hobsbawm and Rudé, 1973, pg. 101)

We may expect elites to respond differently to these different types of protest. One – the traditional local rural protest – threatens damage to local property. The other – action in concert with others in the same social position – implies more persistent social demands.

4.2 Data

We use data on incidents of unrest from Holland (2005), covering each of the 8597 parishes in England over 40 weeks (recorded on 98 individual days) between 28th of June 1830 and 3rd of April 1831. Our outcome is the number of 'large' incidents involving groups of labourers – wage riots, 'robbery', machine-breaking, prisoner rescues, and attacks on local authority figures, as classified in (Tilly, 1995; Aidt et al.,

2022) – where labourers plausibly coordinate across different areas. We model the number of 'large' incidents of unrest within each calendar week as depending upon local time-invariant conditions, plus the number of 'large' incidents in other connected parishes during the week (Eq. 1). We restrict our sample to the 619 parishes that experienced at least one large incident, and remove the effect of local time-invariant conditions by demeaning by parish.

To model link formation between parishes, we use geographic coordinates (latitude and longitude) of each parish centroid from historical maps in Aidt et al. (2022). The key pairwise characteristic is whether two parishes are within 10km of one another – a threshold motivated by documented instances of labourers travelling on foot between nearby parishes (Hobsbawm and Rudé, 1973; Holland, 2005; Aidt et al., 2022). Physical mixing increases the likelihood of mutual influence, though other channels – such as news reports or coach travel – may also play a role. After experimentation, we use tuning parameters $\nu_0 = \frac{1}{30}, \nu_1 = \frac{1}{0.1}$.

Figure 3: Swing incidents in England 1830–31

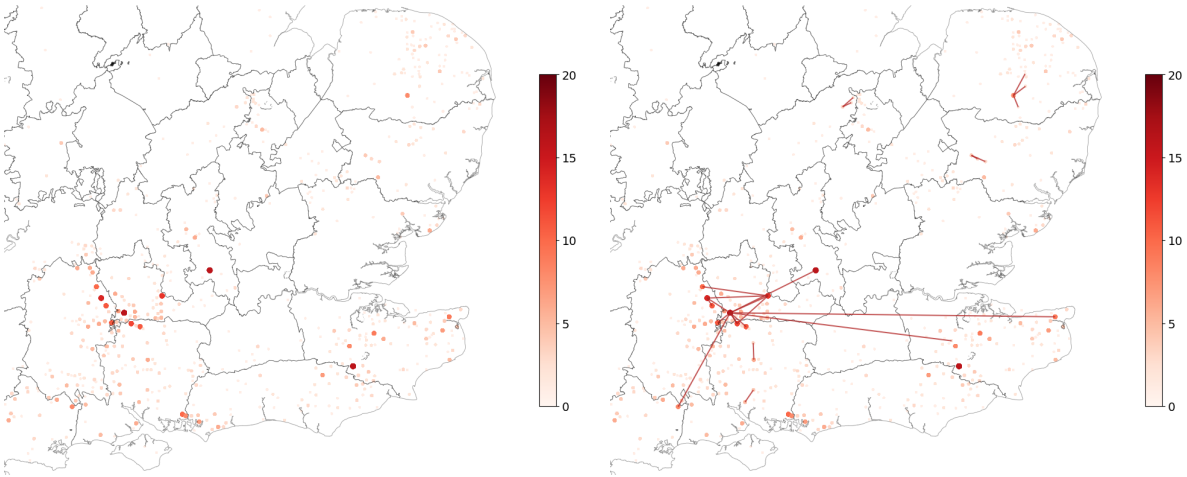

(a) 'Large' incidents, Southeast of England (b) Estimated coordination patterns

4.3 Results

Figure 2 plots our estimated network. The estimated network is very sparse. We only detect 24 non-zero links between 25 distinct parishes. Estimated interaction rates are very small – at $\eta = 0.1$ for labourers within 10km. Our estimated variance of errors is $\hat{\sigma}^2 = 0.09$, compared to a variance in our outcome variables of 0.189. These results suggest that most action was a sporadic response to local conditions, with limited direct influence between parishes outside of the slow spatial diffusion of rioting across England (Aidt et al., 2022). This result is in line with the historical literature, which finds a lack of evidence of coordination between labourers in contrast to contemporaneous urban unrest Hobsbawm and Rudé (1973).

The pattern of influence we find differs across the counties affected by the Swing riots. We find evidence of coordination within nine out of the thirty-nine historic counties of England: Berkshire, Buckinghamshire, Dorset, Hampshire, Kent, Norfolk, Northamptonshire, Suffolk, and Wiltshire. These include five out of the six counties with the most Swing activity – Kent (441 incidents), Norfolk (301 incidents), Wiltshire (259 incidents), Hampshire (255 incidents), and Berkshire (169 incidents).[9] Parishes with many large incidents are central within local interaction networks. The most densely connected area is on the Berskhire-Wiltshire-Hampshire border, with the local network centered on the parish of Kintbury. This also fits with historical evidence – Hobsbawm and Rudé (1973) detail of strong coordinated actions around this border region, describing Kintbury as "a great centre of militancy in 1830".

[9]The missing county is Sussex with (215 incidents).

Matching back to characteristics of parishes detailed in Caprettini and Voth (2020); Aidt et al. (2022) allows us to compute some descriptive evidence about how these connected parishes compare to other parishes that experienced at least one Swing incident. Results are given in Tables 2 and 3.

Table 2: Difference in Swing incidents by estimated coordination

	Number of incidents
Coordinated	5.31
	(1.06)
Intercept	Yes
Observations	969
R^2	0.0222

Notes: Standard errors in parentheses are heteroskedasticity-robust standard errors computed using the HC3 estimator of MacKinnon and White (1985).

Table 3: Coordination by parish-level covariates

	Coordinate	
Enclosure	0.0212	0.0624
	(0.0118)	(0.0347)
Market within 10km	0.0011	−0.0258
	(0.0157)	(0.0298)
Coach stop within 10km	0.0122	0.0437
	(0.0109)	(0.0225)
Newspaper within 10km	0.0319	0.0974
	(0.0214)	(0.0760)
Distance to nearest newspaper	0.0003	0.0052
	(0.0006)	(0.00306)
Threshing machine adoption	0.0092	−0.0296
	(0.0223)	(0.0195)
Demographic controls	No	Yes
Intercept	Yes	Yes
Observations	969	969
R^2	0.0107	0.107

Notes: Standard errors in parentheses are heteroskedasticity-robust standard errors computed using the HC3 estimator of MacKinnon and White (1985).

Parishes that are connected to others experience more incidents of unrest of all types (large and small, not included in our estimation) than disconnected parishes. Looking at characteristics that might lead a parish to influence or be influenced by others, we find that these parishes are more likely to have had common land enclosed and have greater access to newspapers. This is suggestive evidence of newspapers as a mechanism for influence across longer distance. By contrast, we find no difference in the adoption of threshing machines, or access to markets. This distinction suggests different mechanisms causing causes of general unrest, spatial diffusion of information about unrest, and influencing or being influenced by others (Caprettini and Voth, 2020; Aidt et al., 2022).

4.4 Local networks and threat of revolution

Finally, we use our results to separate out the different effect of being exposed to sporadic and coordinated unrest on elite preferences for extending the right to vote. The General Election of 1831 – held after the riots – was called to settle the question of whether parliament should extend the right to vote and reform the electoral system through the Great Reform Act. The proposed reforms lowered property qualifications to vote, still restricting it to a small elite, and reformed the system of borough constituencies. Acemoglu and Robinson (2000, 2001)theorise that fear of revolution by the lower classes led elites to extend the right to vote and reform the electoral system, as a way to credibly commit to reform existing economic and social structure.

To test if there is a different effect of exposure to more coordinated versus sporadic uprisings, we replicate the analysis in Aidt and Franck (2015). Aidt and Franck (2015) establishes that the number of Swing incidents in nearby parishes increased the vote share of the Whigs – the electoral faction that supported extending the right to vote and reforming constituencies – in the 1831 General Election. We extend the analysis by constructing an additional variable for exposure to coordinated unrest – where the constituency centroid is within at least $10km$ of one of the parishes that have at lease one link in our influence network. This is the case in 13 constituencies. To address any concerns about endogeneity of the number of nearby Swing incidents, we replicate both the regular and instrumental variables estimators, using their instrument of distance to the starting point of the first riot in Kent.

Table 4: Exposure to coordinated uprisings and 1831 election results

	Whig share 1831 (%)					
	OLS estimates				IV estimates	
	(1)	(2)	(3)	(4)	(5)	(6)
Riots within 10km	0.569	0.837	0.439	0.596	2.53	3.19
	(0.268)	(0.219)	(0.192)	(0.185)	(0.825)	(1.03)
Coordination within 10km		−27.8		−16.2		−82.8
		(15.4)		(12.5)		(29.1)
Whig share 1826			0.380	0.380	0.143	0.196
			(0.078)	(0.077)	(0.223)	(0.218)
Reform support 1830			12.6	12.1	13.5	10.6
			(5.36)	(5.22)	(6.15)	(6.07)
County constituency			31.6	31.7	40.2	38.2
			(4.97)	(5.04)	(8.80)	(8.72)
University constituency			−61.8	−63.2	−56.3	−52.1
			(20.3)	(21.2)	(13.1)	(13.1)
Patronage index			−15.3	−15.2	−9.06	−8.04
			(3.67)	(3.67)	(4.64)	(4.81)
Declining economy			−10.3	−9.60	−12.8	−16.3
			(6.15)	(6.23)	(6.76)	(6.94)
Spatial controls	No	No	No	No	Yes	Yes
Intercept	Yes	Yes	Yes	Yes	Yes	Yes
Observations	244	244	244	244	244	244
R^2	0.0253	0.0393	0.467	0.472	0.491	0.492

Notes: Controls included to match preferred specifications in Aidt and Franck (2015). In the final two columns, the number of riots within 10km is instrumented by distance to Sevenoaks. For details, see Aidt and Franck (2015). Standard errors in parentheses are heteroskedasticity-robust standard errors computed using the HC3 estimator of MacKinnon and White (1985).

Table 4 gives results from the baseline and preferred specifications in Aidt and Franck (2015), also accounting for the effect of exposure to coordinated unrest. We find two main effects across specification. First, we find a larger effect of exposure to rioting on vote share for the Whigs (0.596 per riot as opposed to 0.439 in the main ordinary least-squares specification, 3.19 per riot as opposed to 2.53 per riot in the instrumental variables specification). This is explained by a large (imprecisely estimated in the ordinary least-squares specifications) negative effect of being exposed to a connected parish in our influence network on vote share for the Whigs. In the preferred specification of Aidt and Franck (2015), the vote share for the Whigs is on average 16.2% lower in constituencies near to at least one connected parish compared to those constituencies with an equivalent amount of uncoordinated rioting. In the instrumental variables specification, the effect is even larger –the vote share for the Whigs is on average 82.8% lower in constituencies near to at least one connected parish compared to those constituencies with an equivalent amount of uncoordinated rioting.

This is suggestive evidence of a polarising effect of different types of unrest on elites. Experience of unrest led elites to prefer to share power more broadly, as predicted by Acemoglu and Robinson (2000). However, experiencing coordinated unrest appears to have led to a reaction amongst local elites against sharing power. Results here are similar to the hardening of anti-reform Tory MPs against franchise expansion in response to contentious gatherings for reform found by Aidt and Franck (2019) in the December 1831 election.

5 Conclusion

Here, we introduce an estimator for unobserved links between individuals from panel data on outcomes and individual characteristics that influence link formation. Our penalised estimator penalises potential links unequally based on these characteristics, penalising links less that are more likely to be present. A fast coordinate-descent algorithm allows a researcher to estimate moderately sized latent networks in reasonable times.

We apply our estimator to estimate patterns of coordination and influence between parishes in the Swing riots of 1830–1831. We find evidence of some patterns of local coordination, especially in the areas around the Berkshire-Hampshire-Wiltshire border. Exposure to different types of unrest appears to have had a polarising effect upon elites. Sporadic unrest made elites more favourable to franchise expansion than previously estimated, but exposure to connected uprisings appears to have hardened elites against franchise expansion.

Our specification excludes direct effects of covariates on others' outcomes through the network, and changes in networks over time (as in De Paula et al., 2024). Further econometric work could extend the estimator to this type of setting.

References

Abaluck, J. and Adams-Prassl, A. (2021). What do Consumers Consider Before They Choose? Identification from Asymmetric Demand Responses*. *The Quarterly Journal of Economics*, 136(3):1611–1663.

Acemoglu, D. and Robinson, J. A. (2000). Why did the west extend the franchose? democracy, inequality, and growth in historical perspective. *Quarterly Journal of Economics*, 115(4):1167–1199.

Acemoglu, D. and Robinson, J. A. (2001). A theory of political transitions. *American Economic Review*, 91(4):938–963.

Aidt, T., Leon-Ablan, G., and Satchell, M. (2022). The social dynamics of collective action: Evidence from the diffusion of the swing riots, 1830–1831. *The Journal of Politics*, 84(1):209–225.

Aidt, T. S. and Franck, R. (2015). Democratization under the threat of revolution: Evidence from the great reform act of 1832. *Econometrica*, 83(2):505–547.

Aidt, T. S. and Franck, R. (2019). What motivates an oligarchic elite to democratize? evidence from the roll call vote on the great reform act of 1832. *The Journal of Economic History*, 79(3):773–825.

Aidt, T. S. and Jensen, P. S. (2013). Workers of the world unite! franchise extensions and the threat of revolution in europe 1820–1938. *European Economic Review*, 72:52–75.

Airoldi, E. M., Costa, T. B., and Chan, S. B. (2013). Stochastic blockmodel approximation of a graphon: Theory and consistent estimation. *Advances in Neural Information Processing Systems*, 26:1–9.

Arkolakis, C., Huneeus, F., and Miyauchi, Y. (2023). Spatial production networks. Working Paper 30954, National Bureau of Economic Research.

Banerjee, A., Chandrasekhar, A., Duflo, E., and Jackson, M. (2013). The Diffusion of Microfinance. *Science*, 341(1236498):363–341.

Barrot, J.-N. and Sauvagnat, J. (2016). Input Specificity and the Propagation of Idiosyncratic Shocks in Production Networks. *The Quarterly Journal of Economics*, 131(3):1543–1592.

Battaglini, M., Crawford, F., Patacchini, E., and Peng, S. (2021). A graphical lasso approach to estimating network connections: the case of us lawmakers. *Mimeo*.

Boucher, V. and Houndetoungan, E. A. (2025). Estimating peer effects using partial network data. *Mimeo*.

Breza, E., Chandrasekhar, A. G., McCormick, T. H., and Pan, M. (2020). Using aggregated relational data to feasibly identify network structure without network data. *American Economic Review*, 110(8):2454–84.

Cai, T., Liu, W., and Luo, X. (2011). A constrained l1 minimization approach to sparse precision matrix estimation. *Journal of the American Statistical Association*, 106(494):594–607.

Calvó-Armengol, A., Patacchini, E., and Zenou, Y. (2009). Peer effects and social networks in education. *The Review of Economic Studies*, 76(4):1239–1267.

Caprettini, B. and Voth, H.-J. (2020). Rage against the machines: Labor-saving technology and unrest in industrializing england. *American Economic Review: Insights*, 2(3):305–20.

Carrell, S. E., Fullerton, R. L., and West, J. E. (2009). Does your cohort matter? measuring peer effects in college achievement. *Journal of Labor Economics*, 27(3):439–464.

Carvalho, V. M., Nirei, M., Saito, Y. U., and Tahbaz-Salehi, A. (2020). Supply Chain Disruptions: Evidence from the Great East Japan Earthquake*. *The Quarterly Journal of Economics*, 136(2):1255–1321.

Chandrasekhar, A. and Lewis, R. (2016). Econometrics of sampled networks. *Mimeo*.

Charlesworth, A. (1979). *Social Protest in Rural Society*. Norwich University Press.

Conley, J. P. and Temimi, A. (2001). Endogenous enfranchisement when groups' preferences conflict. *Journal of Political Economy*, 109(1):79–102.

Currarini, S., Jackson, M. O., and Pin, P. (2009). An economic model of friendship: Homophily, minorities, and segregation. *Econometrica*, 77(4):1003–1045.

De Paula, A. (2017). Econometrics of network models. In B. Honore, A. Pakes, M. P. and Samuelson, L., editors, *Advances in Economics and Econometrics: Theory and Applications: Eleventh World Congress (Econometric Society Monographs,*, Econometric Society Monographs, pages 268–323. Cambridge University Press, Cambridge.

De Paula, A., Rasul, I., and Souza, P. (2024). Identifying network ties from panel data: theory and an application to tax competition. *Review of Economic Studies*, 92(4):1–39.

Fessler, P. and Kasy, M. (2019). How to use economic theory to improve estimators: Shrinking toward theoretical restrictions. *The Review of Economics and Statistics*, 101(4):681–698.

Friedman, J., Hastie, T., and Tibshirani, R. (2007). Sparse inverse covariance estimation with the graphical lasso. *Biostatistics*, 9(3):432–441.

Friedman, J., Hastie, T., and Tibshirani, R. (2010). Regularization Paths for Generalized Linear Models via Coordinate Descent. *Journal of Statistical Software*, 33:1–22.

Gan, L., Narisetty, N. N., and Liang, F. (2019). Bayesian Regularisation for Graphical Models with Unequal Shrinkage. *Journal of the American Statistical Association*, 114(527):1218–1231.

Griffith, A. (2022). Name your friends, but only five? the importance of censoring in peer effects estimates using social network data. *Journal of Labour Economics*, 40(4):779–805.

Griffith, A. and Peng, S. (2024). Identification of network structure in the presence of latent, unobserved factors: a new result using turán's theorem. *Mimeo*.

Hansen, B. E. (2016). Efficient shrinkage in parametric models. *Journal of Econometrics*, 190:115–132.

Hardy, M., Heath, R., Lee, W., and McCormick, T. (2024). Estimating spillovers using imprecisely measured networks. *Arxiv*, `https://arxiv.org/pdf/1904.00136.pdf`.

Hobsbawm, E. J. and Rudé, G. (1973). *Captain Swing*. Penguin Books.

Holland, M. (2005). *Swing Unmasked: The Agricultural Riots of 1830 to 1832 and Their Wider Implications*. Milton Keynes: FACHRS Publications.

Jackson, M. O., Nei, S. M., Snowberg, E., and Yariv, L. (2022). The dynamics of networks and homophily. Working Paper 30815, National Bureau of Economic Research.

Janková, J. and Van de Geer, S. (2018). Inference in high-dimensional graphical models. In Maathuis, M., Drton, M., Lauritzen, S., and Wainwright, M., editors, *Handbook of Graphical Models*, chapter 14, pages 325–351. CRC Press, 1 edition.

König, M. D., Liu, X., and Zenou, Y. (2019). R&D networks: Theory, empirics and policy implications. *Review of Economics and Statistics*, 101(3):476–491.

Lam, C. and Souza, P. (2019). Estimation and selection of spatial weight matrix in a spatial lag model. *Journal of Business and Economic Statistics*, 38(3):693–710.

Lewbel, A., Qu, X., and Tang, X. (2023). Social networks with unobserved links. *Journal of Political Economy*, 131(4):898–946.

Lubold, S., Chandrasekhar, A. G., and McCormick, T. H. (2023). Identifying the latent space geometry of network models through analysis of curvature. *Journal of the Royal Statistical Society Series B: Statistical Methodology*, 85(2):240–292.

MacKinnon, J. G. and White, H. (1985). Some heteroskedasticity-consistent covariance matrix estimators with improved finite sample properties. *Journal of Econometrics*, 29(3):305–325.

Manresa, E. (2013). Estimating the structure of social interactions using panel data. *Mimeo*.

Manski, C. F. (1993). Identification of endogenous social effects: The reflection problem. *The Review of Economic Studies*, 60(3):531–542.

Pouliot, G. (2023). Instrumental variable quantile regression with multivariate endogenous variables. *Mimeo*.

Pouliot, G. (2025). *Optimization-Conscious Econometrics*. Unpublished Manuscript.

Quinault, R. (1994). The french revolution of 1830 and parliamentary reform. *History*, 79(257):377–393.

Ravikumar, P., Wainwright, M. J., Raskutti, G., and Yu, B. (2011). High-dimensional covariance estimation by minimizing l1-penalized log-determinant divergence. *Electronic Journal of Statistics*, 5:935–980.

Rose, C. (2023). Identification of spillover effects using panel data. *Mimeo*.

Ročková, V. and George, E. (2018). The spike-and-slab lasso. *Journal of the American Statistical Association, Theory and Methods*, 113:431–444.

Ročková, V. and George, E. I. (2014). Emvs: The em approach to bayesian variable selection. *Journal of the American Statistical Association*, 109(506):828–846.

Sherman, J. and Morrison, W. (1949). Adjustment of an inverse matrix corresponding to a change in one element of the given matrix. *Annals of Mathematical Statistics*, 20(4):620–624.

Tibshirani, R. (1996). Regression shrinkage and selection via the lasso. *Journal of the Royal Statistical Society: Series B (Methodological)*, 58(1):267–288.

Tilly, C. (1995). *Contention in Great Britain, 1758–1834*. Cambridge: Harvard University Press.

Tseng, P. (2001). Convergence of a block coordinate descent method for nondifferentiable minimization. *Journal of Optimization Theory and Applications*, 109.

Wainwright, M. J. and Jordan, M. I. (2008). *Graphical models, exponential families, and variational inference*. Now Publishers Inc.

Wells, R. (1997). Mr william cobbett, captain swing, and king william iv. *The Agricultural History Review*, 45(1):34–48.

Yuan, M. and Lin, Y. (2007). Model selection and estimation in the gaussian graphical model. *Biometrika*, 94(1):19–35.

Appendix

A1 Example microfoundation

Our data-generating process corresponds to equilibrium outcomes of a game on a network with linear-quadratic utilities and individual-specific consideration sets determined by characteristics (Abaluck and Adams-Prassl, 2021).

Imagine each of $i = 1, ..., N$ individuals on a weighted network G_{ij} who play an action $y_i \in \mathbb{R}_+$. An individual's payoffs depend on their own action and the actions of others through the linear-quadratic utility function

$$u_i = (\beta x_i + \epsilon_i) y_i + \sum_j \gamma_{ij} a_{ij} y_i y_j - \frac{1}{2} y_i^2.$$

There are $T + 1$ periods. In the first period, nature draws a vector-valued position z_i in some vector space $\mathbb{R}_+^M$ for each individual i, covariates x_{it}, and time-varying shocks to marginal benefits ϵ_{it}. Then, each individual forms links with the other at rates η_{z_i,z_j} with interaction intensities γ_{ij}. In the subsequent periods, individuals adjust their actions to maximise their payoffs for the fixed network G. The first-order conditions of this game are

$$(\beta x_{it} + \epsilon_{it}) + \lambda \sum_j \gamma_{ij} a_{ij} y_j - y_i = 0$$

Rearranging

$$y_i^* = (\beta x_i + \epsilon_i) + \lambda \sum_j \gamma_{ij} a_{ij} y_j^*.$$

Stacking this into matrix form and inverting gives

$$y^* = (I - G)^{-1}(X\beta + \epsilon)$$

where $G_{ij} = \gamma_{ij} A_{ij}$ encodes the intensity of interactions between each individual.

A2 Proofs

We start with the following lemma

Lemma 2.

$$\frac{d \log\det(XX')}{dX} = \frac{d \log\det(X'X)}{dX}$$

By determinant rules

$$\begin{aligned} \det(XX') &= \det(X)\det(X') \\ &= \det(X')\det(X) \\ &= \det(X'X). \end{aligned}$$

as $\det(A)$ is a constant. Therefore

$$\frac{d \log\det(XX')}{dX} = \frac{d \log\det(X'X)}{dX}.$$

A2.1 Proposition 1

Proof. Our objective function (fixing $\sigma^2 = 1$ without loss of generality) is

$$l(G) = \log\det\Big(\frac{(I-\gamma G)(I-\gamma G)'}{\sigma^2}\Big) - \operatorname{trace}\Big(S\frac{(I-\gamma G)(I-\gamma G)'}{\sigma^2}\Big) + \sum_{i,j}\ln\Big(\frac{\eta^*_{z_i,z_j}}{2\nu_1}e^{-\frac{|G_{ij}|}{\nu_1}} + \frac{1-\eta^*_{z_i,z_j}}{2\nu_0}e^{-\frac{|G_{ij}|}{\nu_0}}\Big).$$

To show that this is convex, we inspect the second-order subgradients of each term. The second-order subgradient of the first term is

$$2I \otimes S + 2(I-G)^{-1} \otimes (I-G)^{-1}.$$

By construction, $S \succ 0$, and $G \succ 0$. Considering the Neumann series expansion

$$(I-G)^{-1} = \sum_{k=0}^{\infty} G^K$$

as $\rho(G) < 1$. So, $G \succ 0 \implies (I-G)^{-1} \succ 0$. Therefore

$$2I \otimes S + 2(I-G)^{-1} \otimes (I-G)^{-1}$$

is positive semidefinite, which implies that the first term is strictly convex. Now, consider the penalty term. The second-order subdifferential for each ij is (Gan et al., 2019)

$$\frac{\Big(\frac{1}{\nu_0}-\frac{1}{\nu_1}\Big)\frac{\eta_{z_i,z_j}\nu_0}{(1-\eta_{z_i,z_j})\nu_1}e^{(\frac{1}{\nu_0}-\frac{1}{\nu_1})G_{ij}}}{\Big(\frac{\eta_{z_i,z_j}\nu_0}{(1-\eta_{z_i,z_j})\nu_1}e^{(\frac{1}{\nu_0}-\frac{1}{\nu_1})G_{ij}}+1\Big)^2}$$

We can write the subgradient expression as

$$\Big(\frac{1}{\nu_0}-\frac{1}{\nu_1}\Big)\frac{x}{(1+x)^2} \text{ for } x = \frac{\eta_{z_i,z_j}\nu_0}{(1-\eta_{z_i,z_j})\nu_1}e^{(\frac{1}{\nu_0}-\frac{1}{\nu_1})G_{ij}}.$$

For $x > 0$,

$$0 \le \frac{x}{(x+1)^2} \le \frac{1}{4}.$$

Assume that $\nu_1 > \nu_0$ and $\eta_{z_i,z_j} \in [0,1)$. Then $x > 0$, and it follows that

$$0 \ge \frac{\Big(\frac{1}{\nu_0}-\frac{1}{\nu_1}\Big)\frac{\eta_{z_i,z_j}\nu_0}{(1-\eta_{z_i,z_j})\nu_1}e^{(\frac{1}{\nu_0}-\frac{1}{\nu_1})G_{ij}}}{\Big(\frac{\eta_{z_i,z_j}\nu_0}{(1-\eta_{z_i,z_j})\nu_1}e^{(\frac{1}{\nu_0}-\frac{1}{\nu_1})G_{ij}}+1\Big)^2} \le \frac{1}{4}\Big(\frac{1}{\nu_0}-\frac{1}{\nu_1}\Big).$$

These terms are weakly positive. Therefore, if we stack these terms into a $N \times N$ matrix (with zeros on the diagonal as we impose a simple matrix), the result is positive semidefinite. Therefore, the second term is also convex. The sum of convex functions over the same domain is also convex. Therefore, the whole problem is convex.

□

A2.2 Theorem 1

Our proof follows the logic of the proof of the main theorem in Gan et al. (2019). Throughout, we work with the case of $\sigma^2 = 1$ without loss of generality, to lighten notation. The proof proceeds in three steps.

Step 1. Define the set of true links that are 'large enough'

$$\mathcal{B} = \{(i,j) : |G^0_{ij}| > 2(2C_1 + C_3)M_{\Gamma_0}\sqrt{\frac{\ln N}{T}}\},$$

and the set of diagonal entries as $\mathcal{D}$. Construct the set of possible solutions to our problem

$$\underset{G>0,\rho(G)\leq 1, G_{\mathcal{B}^c}=0}{\arg\min} L(G),$$

defined as

$$\mathcal{A} = \{G : (-(I-G)^{-1} + S(I-G))_{\mathcal{B}} + Z_{\mathcal{B}} = 0, G > 0, \rho(G) \leq 1\}.$$

Step 2. Show that $\mathcal{A}$ is nonempty, and there exists an element $\tilde{G} \in \mathcal{A}$ s.t

$$||\tilde{G} - G||_\infty = O_p\Big(\sqrt{\frac{\ln N}{T}}\Big).$$

Step 3 Prove that $\tilde{G}$ is a unique local minimiser of $L(G)$. Therefore, we have that $\tilde{G} = \hat{G}$.

We start by proving the following lemma, that we will use for step 2.

Lemma 3. Define

$$r = \max\Big\{2M_{\Gamma^0}(||\tilde{W}||_\infty + \max(\frac{1}{2}\text{pen}(\delta), \tau), 2(2C_1 + C_3)M_{\Gamma^0}\sqrt{\frac{\ln N}{T}}\Big\}.$$

If

$$\begin{aligned} &r \leq \min\Big\{\frac{1}{3aM_{\Sigma_0}}, \frac{1}{3aM_{\Gamma_0}M^3_{\Sigma_0}}\Big\} \\ &\min|G^0_{\mathcal{B}}| \geq r + \delta \\ &\rho(G_0) \leq 1 \end{aligned}$$

then $\mathcal{A}$ is non-empty and there exists $\hat{G} \in \mathcal{A}$ s.t $||\Delta||_\infty := ||\hat{G} - G_0||_\infty \leq r$.

Proof. To prove this, define the set of true links that are 'large enough'

$$\mathcal{B} = \{(i,j) : |G^0_{ij}| > 2(2C_1 + C_3)M_{\Gamma_0}\sqrt{\frac{\ln N}{T}}\},$$

the set of diagonal entries as $\mathcal{D}$, and

$$\Delta = \hat{G} - G^0.$$

We want to bound $||\Delta||_\infty \leq 2(2C_1 + C_3)M_{\Gamma_0}\sqrt{\frac{\ln N}{T}} \leq r$. From the triangle inequality

$$||\Delta||_\infty = ||\Delta_{\mathcal{B}} + \Delta_{\mathcal{B}^c}||_\infty \leq ||\Delta_{\mathcal{B}}||_\infty + ||\Delta_{\mathcal{B}^c}||_\infty.$$

As the entries of the matrices $\Delta_{\mathcal{B}}, \Delta_{\mathcal{B}^c}$ are in different locations by the definition of the index set,

$$||\Delta_{\mathcal{B}}||_\infty + ||\Delta_{\mathcal{B}^c}||_\infty = \max(||\Delta_{\mathcal{B}}||_\infty, ||\Delta_{\mathcal{B}^c}||_\infty)$$

So, we can sharpen our bound as

$$||\Delta||_\infty \leq \max(||\Delta_{\mathcal{B}}||_\infty, ||\Delta_{\mathcal{B}^c}||_\infty).$$

So we bound $||\Delta||_\infty$ by bounding $||\Delta_{\mathcal{B}}||_\infty$ and $||\Delta_{\mathcal{B}^c}||_\infty$ individually. By definition,

$$\begin{aligned}||\Delta_{\mathcal{B}^c}|| &= \max(\{G^0_{ij} : (i,j) \in \mathcal{B} \cap \mathcal{D}\}) \\ &\leq 2(2C_1 + C_3)M_{\Gamma_0}\sqrt{\frac{\ln N}{T}}.\end{aligned}$$

So, we have to prove that

$$||\Delta_{\mathcal{B}}||_\infty \leq 2(2C_1 + C_3)M_{\Gamma_0}\sqrt{\frac{\ln N}{T}}.$$

Let $\Gamma^0_{\mathcal{B}\mathcal{B}}$ be the $\mathcal{B}, \mathcal{B}$ block of the Hessian of $\text{logdet}((I-G)'(I-G))$, and Z be the matrix of penalisation terms. Define the mapping

$$F(\text{vec}(\Delta_{\mathcal{B}})) = -\Gamma^{-1}_{0,\mathcal{B}\mathcal{B}}\,\text{vec}(H(G_{\prime,\mathcal{B}} + \Delta_{\mathcal{B}})) + \text{vec}(\Delta_{\mathcal{B}}).$$

The function F is continuous. Now $F(\text{vec}(\Delta_{\mathcal{B}})) = \text{vec}(\Delta_{\mathcal{B}})$ at the point where $H(G_{\prime,\mathcal{B}} + \Delta_{\mathcal{B}}) = H(G_{\prime,\mathcal{B}}) = 0$. So, we will prove the result by showing that $F(\mathbb{B}(r)) \subseteq \mathbb{B}(r)$ for the convex and compact l_∞ ball in $\mathbb{R}^{|\mathcal{B}|}$. Then, by Brouwer's fixed point theorem, there exists a fixed point $\text{vec}(\Delta_{\mathcal{B}}) \in \mathbb{B}^r$ i.e $||\Delta_{\mathcal{B}}||_\infty \leq r$.

To show this, let Δ denote the $N \times N$ zero-padded matrix that equals $\Delta_{\mathcal{B}}$ on $\mathcal{B}$ and zero on $\mathcal{B}^c$. Then, we can write

$$\begin{aligned}F(\text{vec}(\Delta_{\mathcal{B}})) &= -\Gamma^{-1}_{0,\mathcal{B}\mathcal{B}}\Big(- (I - G + \Delta)^{-1}_{\mathcal{B}} - (S(I - G + \Delta))_{\mathcal{B}} + Z_{\mathcal{B}}\Big) + \text{vec}(\Delta_{\mathcal{B}}). \\ &= \Gamma^{-1}_{0,\mathcal{B}\mathcal{B}}\Big(- (I - G + \Delta)^{-1}_{\mathcal{B}} + (I - G_0)^{-1} - (I - G_0)^{-1} - (S(I - G + \Delta))_{\mathcal{B}} + Z_{\mathcal{B}}\Big) + \text{vec}(\Delta_{\mathcal{B}}).\end{aligned}$$

As in Gan et al. (2019), we can separate out this expression into two terms

$$F(\text{vec}(\Delta_{\mathcal{B}})) \leq ||\mathbf{I}||_\infty + ||\mathbf{II}||_\infty$$

First, lets bound

$$\begin{aligned}||\mathbf{I}||_\infty &= ||\Gamma^{-1}_{0\mathcal{B}\mathcal{B}}R(\Delta)||_\infty \\ &= M_{\Gamma_0}||R(\Delta)||_\infty.\end{aligned}$$

To bound $||R(\Delta)||_\infty$, note that as Σ_0 is positive semi-definite by definition, it has a unique matrix square root. Therefore, we can bound

$$\begin{aligned}||\Sigma_0^{\frac{1}{2}}||_\infty &= ||\Sigma_0\Sigma_0^{-\frac{1}{2}}||_\infty \\ &\leq ||\Sigma_0||_\infty||\Sigma_0^{-\frac{1}{2}}||_\infty \\ &= ||\Sigma_0||_\infty||(I - G_0)||_\infty \\ &= \leq 2||\Sigma_0||_\infty.\end{aligned}$$

Then, following the steps in the proofs of lemmas 4 and 5 in Ravikumar et al. (2011) exactly, we can bound

$$||M_{\Gamma_0}R(\Delta)||_\infty \leq 3a||\Delta||^2_\infty K^3_{\Sigma_0}$$

where a is the maximum row sum of the matrix of connections A.

Now, by assumption, $\min|G_{\mathcal{B}}| \geq r + \delta$. Therefore, $||\Delta||_\infty \leq r$, $\min|G_{\mathcal{B}}| \geq \delta$, and since $\text{pen}(G)$ is monotonically decreasing we have that $||Z_{\mathcal{B}}||_\infty \leq \text{pen}(\delta)$. It follows that we can write

$$||\mathbf{II}||_\infty \leq M_{\Gamma_0}\Big(||W(I - G_0)||_\infty + \max(\frac{1}{2}\text{pen}(\delta), \tau)\Big)$$

Now, we know from Cai et al. (2011).

$$||W||_\infty \leq C_1\sqrt{\frac{\ln N}{T}}.$$

As $G \succ 0, \rho(G) \leq 1$ we know that $||G_0||_\infty \leq 1$. As G_0 is a simple network by assumption, we have that

$$||I - G_0||_\infty = 1 + ||G_0||_\infty \leq 2.$$

As $||.||_\infty$ is an operator norm, for any A, B

$$||AB||_\infty \leq ||A||_\infty ||B||_\infty.$$

Therefore

$$||W(I - G_0)||_\infty \leq ||W||_\infty ||(I - G_0)||_\infty \leq 2C_1\sqrt{\frac{\ln N}{T}}.$$

Applying the steps in the proof of Theorem A in Gan et al. (2019) under our assumptions on $\frac{1}{T\nu_0}, \frac{1}{T\nu_1}$ gives, for each i, j,

$$\frac{|\text{pen}'_{SS}(\delta)|}{T} < C_3\sqrt{\frac{\ln N}{T}}.$$

Therefore

$$\begin{aligned} 2M_{\Gamma_0}(||W(I - G_0)||_\infty + \max\Big(\frac{|\text{pen}'_{SS}(\delta)|}{T}, \frac{2}{T}\tau\Big) &\leq 2(2C_1 + C_3)M_{\Gamma_0}\sqrt{\frac{\ln N}{T}} \\ &\leq \min\Big\{\frac{1}{3aM_{\Sigma_0}}, \frac{1}{3aM_{\Gamma_0}M_{\Sigma_0}^3}\Big\}. \end{aligned}$$

Therefore, there exists a $\hat{G}$ such that $||\hat{G} - G_0|| \leq r$.

□

Proof of step 2.

Proof. Define the set of true links that are 'large enough'

$$\mathcal{B} = \{(i, j) : |G_{ij}^0| > 2(2C_1 + C_3)M_{\Gamma_0}\sqrt{\frac{\ln N}{T}}\},$$

and the set of diagonal entries as $\mathcal{D}$. Consider the problem

$$\underset{G>0, \rho(G)\leq 1, G_{\mathcal{B}^c}=0}{\arg\min} L(G).$$

Define the solution set as

$$\mathcal{A} = \{G : (-(I - G)^{-1} + S(I - G))_{\mathcal{B}} + Z_{\mathcal{B}} = 0, G > 0, \rho(G) \leq 1\},$$

and the function

$$H(G_{\mathcal{B}}) = -(I - G_{\mathcal{B}})^{-1} + S(I - G_{\mathcal{B}}) + Z_{\mathcal{B}}.$$

$\mathcal{A}$ is the set such that $H(G_{\mathcal{B}}) = 0$.

Define $\min(G^0_{ij}) = 2(2C_1 + C_3)M_{\Gamma_0}\sqrt{\frac{\ln N}{T}}$. $G^0_{ij} \geq 2(2C_1 + C_3)M_{\Gamma_0}\sqrt{\frac{\ln N}{T}}$ if $G^0_{ij} \in \mathcal{B}$, and $G^0_{ij} \leq 2(2C_1 + C_3)M_{\Gamma_0}\sqrt{\frac{\ln N}{T}}$ if $G^0_{ij} \in \mathcal{B}^c \cap \mathcal{D}$.

Now, we want to prove that the set $\mathcal{A}$ is not empty. Define

$$\begin{aligned}
\tilde{W} &= S - \Sigma_0 \\
\Delta &= \hat{G} - G, \\
a &= ||A||_\infty \text{ maximum degree on the binary network} \\
R(\Delta) &= (I - \hat{G})^{-1} - \Sigma_0^{\frac{1}{2}} + \Sigma_0^{\frac{1}{2}}\Delta\Sigma_0^{\frac{1}{2}},
\end{aligned}$$

the difference between the gradient of $\text{logdet}((I - \hat{G})(I - \hat{G}))$ and the first-order Taylor expansion of the gradient about G_0. Now, we apply our lemma. To apply this, we must verify the conditions for the lemma. Consider

$$r = 2(2C_1 + C_3)M_{\Gamma_0}\sqrt{\frac{\ln N}{T}}.$$

Therefore $\min|G^0_{ij}| > r + \delta$. Furthermore, given our conditions on the sample size, the condition on r also holds. Therefore

$$||\hat{G} - G_0||_\infty \leq 2(2C_1 + C_3)M_{\Gamma_0}\sqrt{\frac{\ln N}{T}}.$$

To convert this into a Frobenius norm bound, we note that there are at most a non-zero entries

$$||\hat{G} - G_0||_F \leq 2\sqrt{a}(2C_1 + C_3)M_{\Gamma_0}\sqrt{\frac{\ln N}{T}}.$$

□

Proof of step 3.

Proof. Finally, we need to verify that $\hat{G}$ is a local minimiser of the loss function. We do thus by showing that

$$L(\hat{G} + \Delta) - L(\hat{G}) \geq 0$$

for some $||\Delta||_\infty \leq \epsilon$. To do this, split our loss function into

$$\begin{aligned}
(1) &= \log\det\Big(\frac{(I - \gamma G)(I - \gamma G)'}{\sigma^2}\Big) - \text{trace}\Big(S\frac{(I - \gamma G)(I - \gamma G)'}{\sigma^2}\Big) \\
(2) &= \sum_{i,j} \ln\Big(\frac{\eta^*_{z_i,z_j}}{2\nu_1}e^{-\frac{|G_{ij}|}{\nu_1}} + \frac{1 - \eta^*_{z_i,z_j}}{2\nu_0}e^{-\frac{|G_{ij}|}{\nu_0}}\Big).
\end{aligned}$$

Applying lemma A.5 in Battaglini et al. (2021) gives that this is greater than zero. Now we need to bound the deviation in the penalty term (B). The same argument as in the bound of the fraction in (B) step 3 in Theorem A. in Gan et al. (2019) is sufficient to bound this term as greater than zero. So, our result follows. □

Finally, we need to show the results for the values of C_1 given the different tail conditions on the distribution of ϵ. We can take these directly from the results bounding the deviation of $||W||_\infty$ in Cai et al. (2011).

A2.3 Proposition 2

Proof. Our algorithm is a block-coordinate descent algorithm over a function that is separable into a differentiable and non-differentiable part. To start with, we repeat a result from Tseng (2001). Consider a function

$$f(x) = g(x) + \sum_i h(x_i)$$

where $g(x)$ is a convex, differentiable, and single-valued function over its domain, and $h(x_i)$ is convex and non-differentiable for each x_i. Then a block-coordinate descent algorithm converges to the true optimum of $f()$.

Split our optimisation problem Eq. 9 into two parts

$$\log\det\Big(\frac{(I-\gamma G)(I-\gamma G)'}{\sigma^2}\Big) - \text{trace}\Big(S\frac{(I-\gamma G)(I-\gamma G)'}{\sigma^2}\Big), \text{ and}$$
$$\sum_{i,j} \ln\Big(\frac{\eta^*_{z_i,z_j}}{2\nu_1}e^{-\frac{|G_{ij}|}{\nu_1}} + \frac{1-\eta^*_{z_i,z_j}}{2\nu_0}e^{-\frac{|G_{ij}|}{\nu_0}}\Big).$$

From the proof of proposition 1, we see that the first part is a convex, differentiable, and single-valued function over the domain $\rho(G) < 1$. Furthermore, we see that the second part is convex and non-differentiable over the domain $\rho(G) < 1$. So, we can apply the result from Tseng (2001) to show that a block-coordinate descent algorithm will converge.

□